applied sciences

MDPI

Communication

Broadband Tunable Passively Q-Switched Erbium-Doped ZBLAN Fiber Laser Using Fe_3O_4-Nanoparticle Saturable Absorber

Kaidi Cai [1,2], Xin Zhang [1,*], Xi Wang [3], Cunzhu Tong [1] and Lijun Wang [1]

[1] State Key Laboratory of Luminescence and Applications, Changchun Institute of Optics, Fine Mechanics and Physics, Chinese Academy of Sciences, Changchun 130033, China
[2] Center of Materials Science and Optoelectronics Engineering, University of Chinese Academy of Sciences, Beijing 100049, China
[3] Center for the Physics of Low-Dimensional Materials, Henan Joint International Research Laboratory of New Energy Materials and Devices, School of Physics and Electronics, Henan University, Kaifeng 475001, China
* Correspondence: zhang315xin@ciomp.ac.cn

Featured Application: Spectroscopic, sensing, material processing, and laser surgery.

Abstract: We experimentally demonstrate a passively Q-switched wavelength tunable 2.8 μm erbium-doped fiber laser. Fe_3O_4 nanoparticles deposited on a gold mirror are used as a saturable absorber (SA). Stable Q-switched pulses within the tunable range of 2710–2810 nm are obtained. At the wavelength of 2760 nm, a maximum Q-switched output power of 188 mW is achieved with a repetition rate of 115.8 kHz and a pulse width of 1.3 μs. The corresponding pulse energy is 1.68 μJ. This demonstration shows the ability of Fe_3O_4 to function as a broadband mid-infrared SA.

Keywords: fiber laser; ZBLAN laser; mid-infrared

Citation: Cai, K.; Zhang, X.; Wang, X.; Tong, C.; Wang, L. Broadband Tunable Passively Q-Switched Erbium-Doped ZBLAN Fiber Laser Using Fe_3O_4-Nanoparticle Saturable Absorber. *Appl. Sci.* **2022**, *12*, 9168. https://doi.org/10.3390/app12189168

Academic Editor: Christian Spielmann

Received: 29 July 2022
Accepted: 10 September 2022
Published: 13 September 2022

1. Introduction

A laser of around 3 μm has attracted much attention in national defense and security, laser surgery, frequency conversion, greenhouse gas monitoring, and spectroscopy [1–6]. Some applications, such as material processing, require high-power pulse laser sources to melt materials and tunable wavelengths to match the absorption peak of different materials. Additionally, for several spectroscopic and sensing applications, a tunable light source is needed. Q-switched erbium-doped ZBLAN fibers are a promising method to generate pulsed and tunable lasers around 3 μm because erbium-doped ZBLAN fibers have made great progress in recent years in high-power output fields [7–9], and the emission band of erbium ion is relatively wide [10]. Compared to active Q-switching, passive schemes do not need any externally controlled modular. Instead, a saturable absorber (SA) is used to generate a pulse. The SA has an intensity-related absorption rate of the laser. The unsaturated SA absorbs light and forms a high Q-factor laser cavity. After saturation, the absorption rate of SA is greatly reduced, and the Q-factor of the cavity is declined. Passive Q-switching is more economical and more attractive. Recently, many passively Q-switched pulsed fiber lasers around 3 μm were reported. Different kinds of SAs were used to modulate the cavity loss. Besides traditional bulk SA modulators, such as semiconductor saturable absorber mirrors (SESAM) [11–14] and Fe^{2+}:ZnSe crystals [15], two-dimensional (2D) materials are widely investigated, including graphene [16,17], black phosphorous [18], topological insulator [19,20], magnetite (Fe_3O_4) [21,22], antimonene [23], transmission metal dichalcogenides [24,25], and gold nanorods [26].

While SESAM is widely used for its mature manufacturing process and customized properties, the cost of production is high. Additionally, the operating wavelength is typically narrow, which is not suitable for wavelength-tunable applications. Thus far, many

wavelength tunable Q-switched lasers around 2.8 μm based on 2D SAs have been demonstrated, as shown in Table 1. However, demonstrations in the mid-infrared wavelength are seldom. Among reports in the near-infrared wavelength range, the majority of average output power is low, and the tunable bandwidth is below 48 nm. In 2020, a tunable Q-switched laser based on Fe_3O_4-nanoparticle SA was reported, and the wavelength was tunable from 2812.4 nm to 3031.6 nm, corresponding to a range of 219.2 nm [22]. Fe_3O_4 is a suitable material to serve as a broadband mid-infrared Q-switcher. However, this report was demonstrated on a dysprosium (Dy^{3+}) doped ZBLAN fiber. Dy^{3+}-doped fiber can deliver a much longer wavelength tuning range [27]. However, the $^6H_{13/2} \rightarrow {}^6H_{15/2}$ transition of Dy^{3+} ion has a significantly lower emission cross-section than the $^4I_{11/2} \rightarrow {}^4I_{13/2}$ transition of Er^{3+} ion [28], which is detrimental to high power usage. For the typical usage of a Q-switched pulsed laser, a higher pulse energy is important.

Table 1. Passively Q-switched wavelength-tunable fiber lasers.

SA	Dopant	Wavelength (nm)	Average Power (mW)	Pulse Energy (nJ)	Ref.
Graphene	Er^{3+}	1547–1557	4	160	[16]
MoS_2	Er^{3+}	1519–1567	5.91	160	[29]
MoS_2	Er^{3+}	1484–1492	0.8	1.2	[30]
Black phosphorus	Yb^{3+}	1040–1045	8.9	141.27	[31]
Fe_3O_4	Dy^{3+}	2812–3032	111	900	[22]
Fe_3O_4	Er^{3+}	2710–2810	188	1680	This work

In this article, a broadband-tunable passively Q-switched erbium-doped ZBLAN fiber laser is demonstrated using a Fe_3O_4 saturable absorber mirror (SAM). The SAM is fabricated via depositing Fe_3O_4-nanoparticles on a gold mirror. A refractive blazed grating is used to tune the wavelength. The wavelength tunable bandwidth is measured to be 100 nm. The Q-switched output power reaches a maximum of 188 mW at the wavelength of 2760 nm. The output characteristics with the varied pump power and wavelength are investigated.

2. Experiment

A schematic diagram of the Q-switched wavelength-tunable fiber laser is shown in Figure 1. A laser diode with a pigtail fiber is used as the pump source. The diode is water-cooled and operated at a wavelength of 976 nm under a continuous wave (CW) regime. The output fiber of the diode has a core diameter of 105 μm and a numerical aperture (NA) of 0.22. The pump laser is collimated by an aspheric lens L1 (f = 10 mm, ϕ = 12.7 mm, NA = 0.54) and coupled into the active fiber by a plano-convex lens L2 (f = 20 mm, ϕ = 12.7 mm). The active fiber is a 70,000 ppm Er^{3+}:ZBLAN fiber fabricated by Le Verre Fluoré. The fiber is 3 m in length and has a core diameter of 15 μm with a NA of 0.12. The inner cladding of the fiber is a truncated circular (double D-shaped) cladding with a short/long diameter of 240/260 μm and an NA of 0.46. The outer circular cladding is 290 μm in diameter. Both ends of the fiber are cleaved at an angle of about 10° to avoid any parasitic oscillation. The output laser is collimated by L3 (same lens as L2) and split by a germanium plate. The laser that passes through the germanium plate is reflected by a blazed grating (GR25-0616, Thorlabs). On the other side of the cavity, a dichroic mirror coated with reflectivity R > 99.9% at 2800 nm and transmissivity T > 98.0% at 976 nm for a 45° angle reflects the 2.8 μm laser beam, which is focused on the Fe_3O_4 SAM by L4 (same lens as L2).

The refractivity of the germanium plate at a 45° angle is measured to be about 47.7%, which is also the coupling ratio of the output 1. Output 2 is captured by a photoconductive detector (PVI-4TE-5, VIGO System) together with a 1-GHz-bandwidth oscilloscope (MOD3104, Tektronix) to make sure the measurements are conducted in the stable Q-switching mode. By tuning the angle of the grating, the output wavelength is tunable. Power and spectrum are measured from output 1, with a thermoelectricity power meter (S314C, Thorlabs) and a Fourier transform spectrometer (OSA207, Thorlabs) separately.

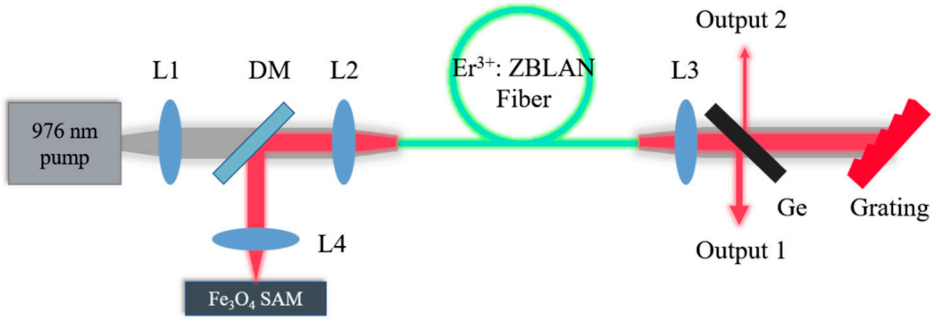

Figure 1. Experimental setup for Q-switched wavelength-tunable fiber laser. L1, aspheric lens; L2, L3, L4, plano-convex lenses; DM, dichroic mirror; Ge, germanium plate.

3. Results and Discussions

The grating was first tuned to maximize the power of the laser output. The Q-switched 2.8 μm laser was demonstrated, and the pulse was measured and shown in Figures 2 and 3. Figure 2 shows the output power as a function of pump power. At a pump power of 0.13 W, a 2.8 μm laser is emitted and operated under the CW regime. As the pump power increases beyond 0.98 W, a stable Q-switching regime is achieved. Additionally, as the pump power further increases to 9.6 W, mode locking is realized. A pump power higher than 14.5 W brings about thermal damage to the SAM, and the maximum output power is measured to be 295 mW. The output power increases almost linearly with the pump power, and the slope efficiency is fitted to be 2.0%.

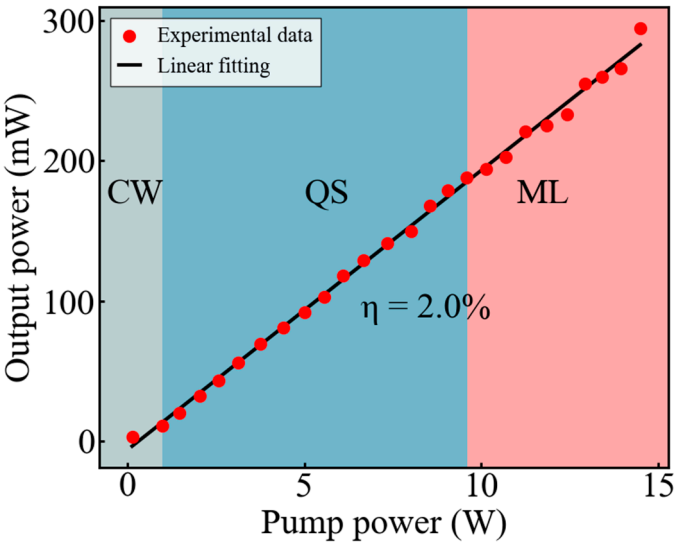

Figure 2. Output power as a function of pump power. CW, continuous wave; QS, Q-switching; ML, mode locking.

At a pump power of 0.98 W, the Q-switched pulse appears first, with a repetition rate of 10.92 kHz and a pulse width of 4.6 μs, as shown in Figure 3a. As the pump power increases, the Q-switching regime is stable until 9.6 W of pump power, corresponding to a repetition rate of 115.8 kHz and a pulse width of 1.3 μs, shown in Figure 3b. At higher pump power, the intensity of pulse trains is more stable, and the single pulse envelope is cleaner. This change suggests the Q-switching is more stable, and the self-mode locking is restrained at higher pump power. At 9.6 W of pump power, the optical and RF spectrum of the laser is measured and shown in Figure 3c,d. The FWHM of the laser spectrum is 0.1 nm. A free-running 2.8 μm CW laser spectrum is measured at about the same output power, which is 188 mW, and the FWHM is 0.45 nm. The compression of the spectrum is caused by the spectrum sensitively grating in the laser cavity. The signal-to-noise ratio (SNR) of

the laser is about 35 dB, which is typical for stable passive Q-switching [16,18,26]. The laser cavity has SAM in one end and grating in another; thus, the reflectivity of the cavity is high. A high inter-cavity laser energy causes obvious side noise in the RF spectrum.

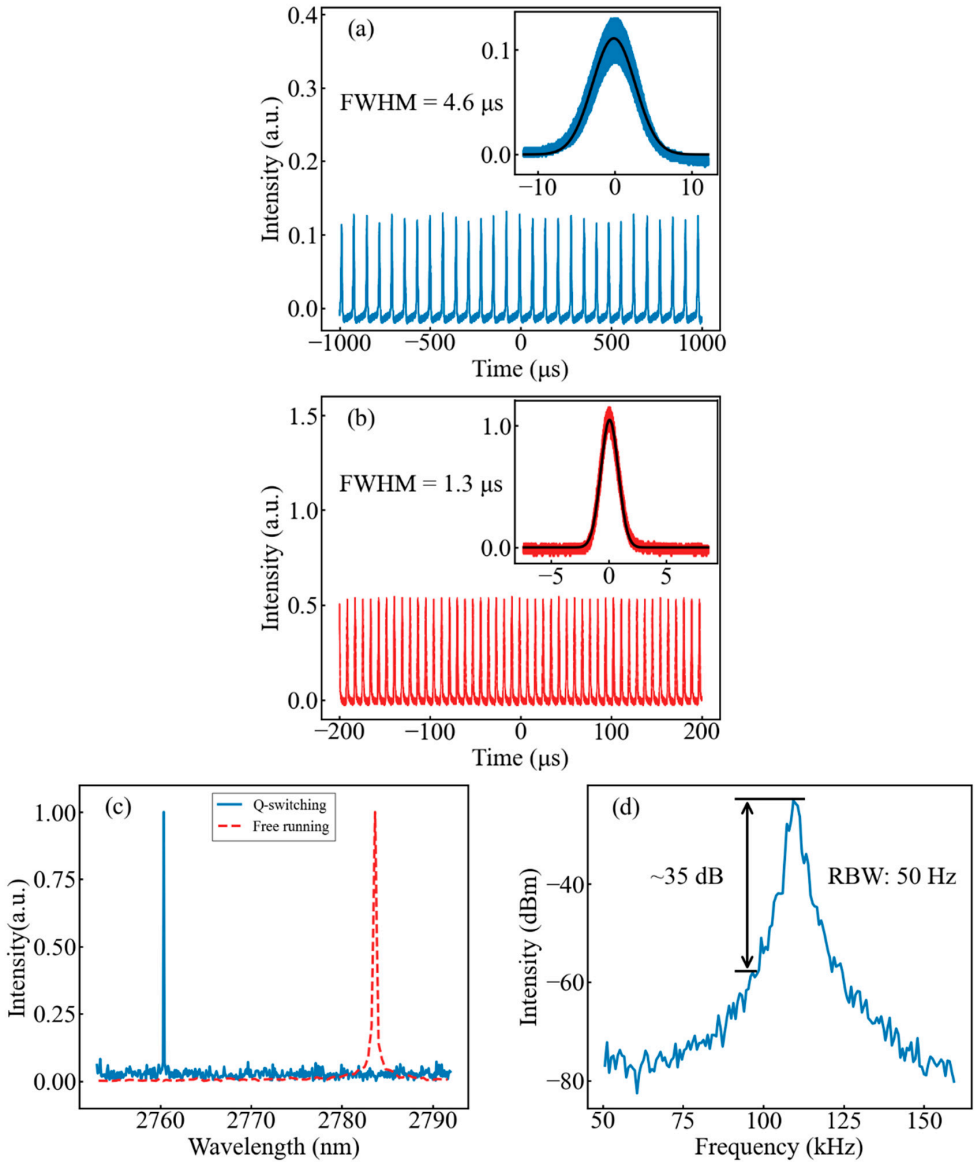

Figure 3. Q-switched laser pulse trains and single pulse envelope at a pump power of (**a**) 0.98 W and (**b**) 9.6 W. (**c**) Optical spectrum of Q-switched laser and free running laser in linear scale at a pump power of 9.6 W. (**d**) RF spectrum of Q-switched laser at a pump power of 9.6 W, measured with a resolution bandwidth (RBW) of 30 Hz.

Figure 4 shows the evolution of the output pulses as a function of the pump power, corresponding to the QS area of Figure 2. Figure 4a shows that as the pump power increases from 0.98 to 9.6 W, the repetition rate increases from 10.92 to 115.8 kHz, and the pulse width of the laser pulse decreases from 3.7 to 1. 3 μs. Figure 4b shows that within the same pump power range, the peak power increases from 0.27 to 1.27 W, and the pulse energy increases from 1.01 to 1.68 μJ. Continuous increases in the pump power lead to the mode-locking regime of the laser, as shown in Figure 5. The repetition rate of the mode-locking pulse is 32.77 MHz, which is determined by the effective cavity length. This configuration contains a 3-m-long fiber and a 15-cm-long external cavity. The refractive index of the fiber core is 1.483, according to the fiber manufacturer. Thus, the effective length is 4.6 m, corresponding

to a theoretical repetition rate of 32.6 MHz given by $c/2L_{eff}$, where c is the speed of light and L_{eff} is the effective length of the fiber cavity. The insert shows that the mode-locked pulses have a shorter rising edge than the falling edge. Before the pump power increases higher than 14.5 W, the Q-switched state can be brought back by decreasing the pump power, suggesting that the SAM is not damaged. The RF spectrum is measured and shown in Figure 5b. The SNR is about 55 dB, indicating a stable mode-locking regime.

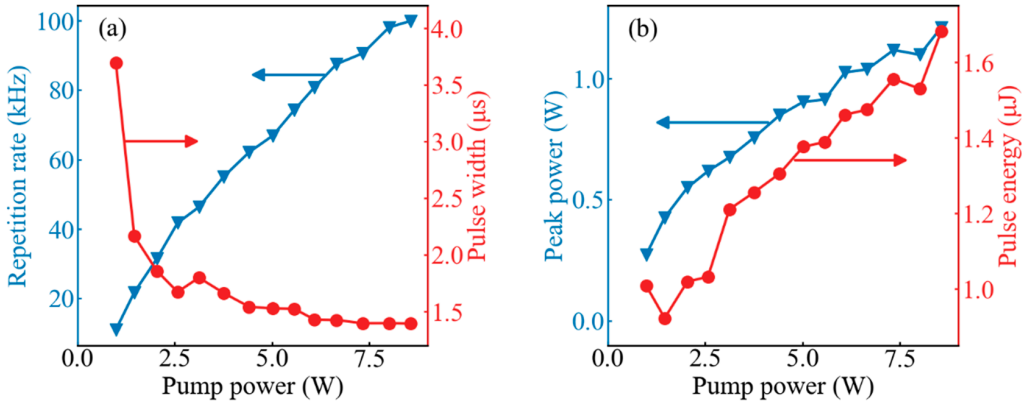

Figure 4. (**a**) Repetition rate (triangle) and pulse width (circle) as a function of pump power. (**b**) Peak power (triangle) and pulse energy (circle) as a function of pump power.

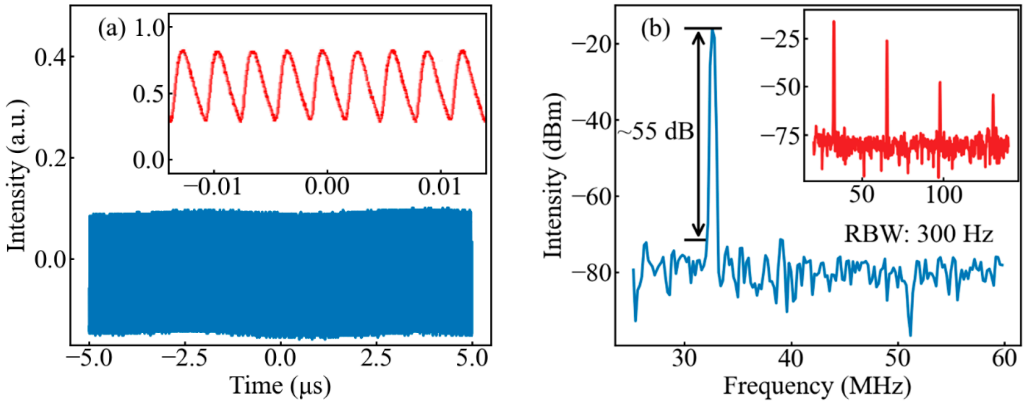

Figure 5. (**a**) Laser pulse trains in 10 μs and 0.028 μs time durations at a pump power of 10.7 W. (**b**) The RF spectrum at a pump power of 10.7 W, measured with a RBW of 300 Hz.

By tuning the angle of the grating, a wavelength tunable Q-switched laser is achieved, as shown in Figure 6a. The wavelength is tunable from 2710 to 2810 nm. At a pump power of 1.4 W, the output power changes from 85 to 104 mW. The peak power is measured at a wavelength of 2760 nm, which is also the center of the tunable range. The power variations are caused by the gain of Er^{3+} ions; see Appendix A, Figure A1. For our setup, the gain of the fiber is maximum at 2760 nm. The gain decreases as the spectrum increases and decreases, eventually becoming not high enough outside the tunable range. Figure 6b shows that as the wavelength increases, the repetition rate of the pulse decreases while the pulse width increases. In previous reports of wavelength tunable Q-switched lasers, with the increase in output wavelength, the repetition range increases and then decreases, while the pulse width has an opposite trend [22,26]. The potential reason is that the SAMs have different saturation intensity at different wavelengths.

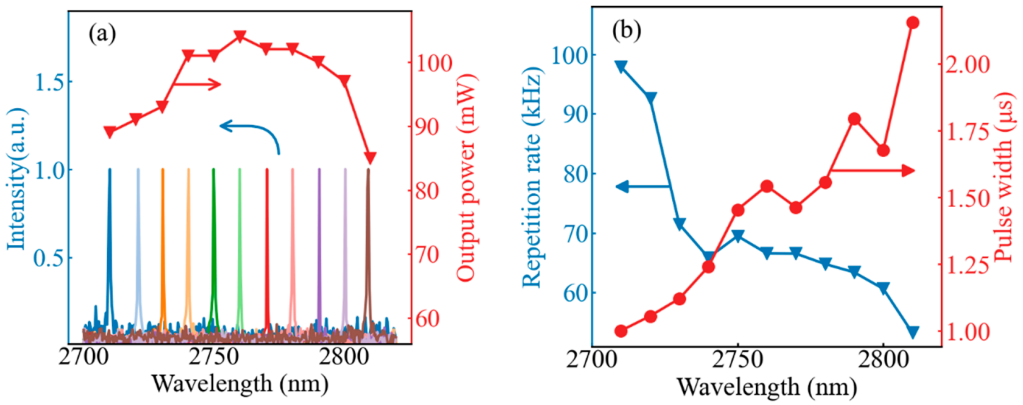

Figure 6. (**a**) Output spectrum (colored lines) and output power (triangle) as a function of wavelength at a pump power of 1.4 W. (**b**) Repetition rate (triangle) and pulse width (circle) as a function of wavelength at a pump power of 1.4 W.

4. Conclusions

In conclusion, we demonstrated a passively Q-switched tunable Er^{3+}:ZBLAN fiber laser around 2.8 μm. A Fe_3O_4-nanoparticle SAM is used as an efficient broadband mid-infrared Q-switcher. Stable Q-switched pulses are observed with a tunable wavelength of 2710–2810 nm. At a wavelength of 2760 nm, a maximum output power of 188 mW is obtained with a repetition rate of 115.8 kHz and a pulse width of 1.3 μs. The corresponding pulse energy is 1.68 μJ. The wavelength-tunable ability is helpful for applications such as material processing and laser surgery since the output can be tuned to match the absorption peak of different materials. This demonstration shows that Fe_3O_4 nanoparticles are a promising broadband SA material for the mid-infrared region.

Author Contributions: Conceptualization, K.C. and X.Z.; methodology, K.C., X.Z. and X.W.; validation, K.C.; formal analysis, K.C.; investigation, K.C., X.Z. and X.W.; resources, C.T.; data curation, K.C.; writing—original draft preparation, K.C.; writing—review and editing, K.C., X.Z., C.T. and L.W.; visualization, K.C.; supervision, C.T. and L.W.; project administration, C.T. and L.W.; funding acquisition, C.T. All authors have read and agreed to the published version of the manuscript.

Funding: This research was funded by the National Natural Science Foundation of China (61790584 and 62025506).

Institutional Review Board Statement: Not applicable.

Informed Consent Statement: Not applicable.

Data Availability Statement: Not applicable.

Acknowledgments: K. Cai would like to thank Regan for helping with the grammar.

Conflicts of Interest: The authors declare no conflict of interest.

Appendix A

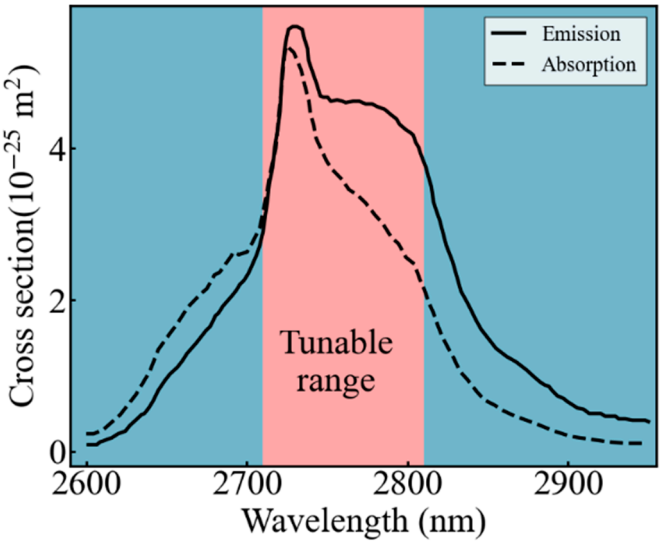

Figure A1. The emission and absorption cross-section of Er^{3+} as a function of emission wavelength. Experimental data from [28].

References

1. Jackson, S.D. Towards high-power mid-infrared emission from a fibre laser. *Nature Photon.* **2012**, *6*, 423–431. [CrossRef]
2. Jackson, S.D.; Jain, R.K. Fiber-based sources of coherent MIR radiation: Key advances and future prospects (invited). *Opt. Express* **2020**, *28*, 30964–31019. [CrossRef] [PubMed]
3. Walsh, B.M.; Lee, H.R.; Barnes, N.P. Mid infrared lasers for remote sensing applications. *J. Lumin.* **2016**, *169*, 400–405. [CrossRef]
4. Kottmann, J.; Grob, U.; Rey, J.M.; Sigrist, M.W. Mid-Infrared Fiber-Coupled Photoacoustic Sensor for Biomedical Applications. *Sensors* **2013**, *13*, 535–549. [CrossRef] [PubMed]
5. Ebrahim-Zadeh, M.; Vodopyanov, K. Mid-infrared coherent sources and applications: Introduction. *J. Opt. Soc. Am. B* **2016**, *33*, MIC1. [CrossRef]
6. You, Z.; Li, J.; Wang, Y.; Chen, H.; Zhu, Z.; Tu, C. Spectroscopic and laser properties of Er: LuGG crystal at ~2.8 μm. *Appl. Phys. Express* **2019**, *12*, 052019. [CrossRef]
7. Tokita, S.; Murakami, M.; Shimizu, S.; Hashida, M.; Sakabe, S. Liquid-cooled 24 W mid-infrared Er: ZBLAN fiber laser. *Opt. Lett.* **2009**, *34*, 3062. [CrossRef]
8. Fortin, V.; Bernier, M.; Bah, S.T.; Vallée, R. 30 W fluoride glass all-fiber laser at 2.94 μm. *Opt. Lett.* **2015**, *40*, 2882. [CrossRef]
9. Aydin, Y.O.; Fortin, V.; Vallée, R.; Bernier, M. Towards power scaling of 2.8 μm fiber lasers. *Opt. Lett.* **2018**, *43*, 4542. [CrossRef]
10. Wang, W.C.; Zhou, B.; Xu, S.H.; Yang, Z.M.; Zhang, Q.Y. Recent advances in soft optical glass fiber and fiber lasers. *Prog. Mater. Sci.* **2019**, *101*, 90–171. [CrossRef]
11. Li, K.H.; Ma, Z.; Choi, H.W. Single-mode whispering gallery lasing from metal-clad GaN nanopillars. *Opt. Lett.* **2012**, *37*, 374–376. [CrossRef] [PubMed]
12. Li, J.; Hudson, D.D.; Liu, Y.; Jackson, S.D. Efficient 2.87 μm fiber laser passively switched using a semiconductor saturable absorber mirror. *Opt. Lett.* **2012**, *37*, 3747–3749. [CrossRef] [PubMed]
13. Haboucha, A.; Fortin, V.; Bernier, M.; Genest, J.; Messaddeq, Y.; Vallée, R. Fiber Bragg grating stabilization of a passively mode-locked 2.8 μm Er^{3+}: Fluoride glass fiber laser. *Opt. Lett.* **2014**, *39*, 3294–3297. [CrossRef] [PubMed]
14. Shen, Y.; Wang, Y.; Luan, K.; Huang, K.; Tao, M.; Chen, H.; Yi, A.; Feng, G.; Si, J. Watt-level passively Q-switched heavily Er^{3+}-doped ZBLAN fiber laser with a semiconductor saturable absorber mirror. *Sci. Rep.* **2016**, *6*, 26659. [CrossRef]
15. Wei, C.; Zhu, X.; Norwood, R.A.; Peyghambari, N. Passively continuous-wave mode-locked Er^{3+}-doped ZBLAN fiber laser at 2.8 μm. *Opt. Lett.* **2012**, *37*, 3849–3851. [CrossRef]
16. Wei, C.; Zhu, X.; Wang, F.; Xu, Y.; Balakrishnan, K.; Song, F.; Norwood, R.A.; Peyghambarian, N. Graphene Q-switched 2.78 μm Er3+-doped fluoride fiber laser. *Opt. Lett.* **2013**, *38*, 3233–3236. [CrossRef]
17. Tokita, S.; Murakami, M.; Shimizu, S.; Hashida, M.; Sakabe, S. Graphene Q-switching of a 3 μm Er: ZBLAN fiber laser. In Proceedings of the Advanced Solid-State Lasers Congress, Paris, France, 27 October 2013. [CrossRef]
18. Qin, Z.; Xie, G.; Zhang, H.; Zhao, C.; Yuan, P.; Wen, S.; Qian, L. Black phosphorus as saturable absorber for the Q-switched Er:ZBLAN fiber laser at 2.8 μm. *Opt. Express* **2015**, *23*, 24713–24718. [CrossRef]
19. Li, J.; Luo, H.; Wang, L.; Zhao, C.; Zhang, H.; Li, H.; Liu, Y. 3-μm mid-infrared pulse generation using topological insulator as the saturable absorber. *Opt. Lett.* **2015**, *40*, 3659–3662. [CrossRef]

20. Tang, P.; Wu, M.; Wang, Q.; Miao, L.; Huang, B.; Liu, J.; Zhao, C.; Wen, S. 2.8 μm pulsed Er^{3+}:ZBLAN fiber laser modulated by topological insulator. *IEEE Photon. Technol. Lett.* **2016**, *28*, 1573–1576. [CrossRef]
21. Bai, X.; Mou, C.; Xu, L.; Wang, S.; Pu, S.; Zeng, X. Passively Q-switched erbium-doped fiber laser using Fe_3O_4-nanoparticle saturable absorber. *Appl. Phys. Express* **2016**, *9*, 042701. [CrossRef]
22. Yang, J.; Hu, J.; Luo, H.; Li, J.; Liu, J.; Li, X.; Liu, Y. Fe_3O_4 nanoparticles as a saturable absorber for a tunable Q-switched dysprosium laser around 3 μm. *Photon. Res.* **2020**, *8*, 70–77. [CrossRef]
23. Luo, H.; Tian, X.; Gao, Y.; Wei, R.; Li, J.; Qiu, J.; Liu, Y. Antimonene: A long-term stable two-dimensional saturable absorption material under ambient conditions for the mid-infrared spectral region. *Photon. Res.* **2018**, *6*, 900–907. [CrossRef]
24. Wei, C.; Luo, H.; Zhang, H.; Li, C.; Xie, J.; Li, J.; Liu, Y. Passively Q-switched mid-infrared fluoride fiber laser around 3 μm using a tungsten disulfide (WS_2) saturable absorber. *Laser Phys. Lett.* **2016**, *13*, 105108. [CrossRef]
25. Wang, S.; Tang, Y.; Yang, J.; Zhong, H.; Fan, D. MoS_2 Q-switched 2.8 μm Er:ZBLAN fiber laser. *Laser Phys.* **2019**, *29*, 025101. [CrossRef]
26. Luo, H.; Kang, Z.; Gao, Y.; Peng, H.; Li, J.; Qin, G.; Liu, Y. Large aspect ratio gold nanorods (LAR-GNRs) for mid-infrared pulse generation with a tunable wavelength near 3 μm. *Opt. Express* **2019**, *27*, 4886–4896. [CrossRef]
27. Majewski, M.R.; Woodward, R.I.; Jackson, S.D. Dysprosium-doped ZBLAN fiber laser tunable from 2.8 μm to 3.4 μm, pumped at 1.7 μm. *Opt. Lett.* **2018**, *43*, 971–974. [CrossRef] [PubMed]
28. Jackson, S.D.; Lancaster, D.G. Fibre lasers that bridge the shortwave to midwave regions of the infrared spectrum. In *Fiber Lasers*; Editor, O.G., Ed.; Okhotnikov; Wiley-VCH Verlag GmbH & Co. KGaA: Weinheim, Germany, 2012; pp. 233–267. [CrossRef]
29. Huang, Y.; Luo, Z.; Li, Y.; Zhong, M.; Xu, B.; Che, K.; Xu, H.; Cai, Z.; Peng, J.; Weng, J. Widely-tunable, passively Q-switched erbium-doped fiber laser with few-layer MoS_2 saturable absorber. *Opt. Express* **2014**, *22*, 25258–25266. [CrossRef]
30. Ahmad, H.; Ismail, M.A.; Suthaskumar, M.; Tiu, Z.C.; Harun, S.W.; Zulkifli, M.Z.; Samikannu, S.; Sivaraj, S. S-band Q-switched fiber laser using molybdenum disulfide (MoS_2) saturable absorber. *Laser Phys. Lett.* **2016**, *13*, 035103. [CrossRef]
31. Song, H.; Wang, Q.; Wang, D.; Li, L. Passively Q-switched wavelength-tunable 1-μm fiber lasers with tapered-fiber-based black phosphorus saturable absorbers. *Results Phys.* **2018**, *8*, 276–280. [CrossRef]